51st IEEE Conference on Decision and Control
December 10-13, 2012. Maui, Hawaii, USA

Turbulent drag reduction by streamwise traveling waves

Armin Zare, Binh K. Lieu, and Mihailo R. Jovanović

***Abstract*— For a turbulent channel flow with zero-net-mass-flux surface actuation in the form of streamwise traveling waves we develop a model-based approach to design control parameters that can reduce skin-friction drag. In contrast to the traditional approach that relies on numerical simulations and experiments, we use turbulence modeling in conjunction with stochastically forced linearized equations to determine the effect of small amplitude traveling waves on the drag. Our simulation-free approach is capable of identifying drag reducing trends in traveling waves with various control parameters. High-fidelity simulations are used to verify quality of our theoretical predictions.**

***Index Terms*— Drag reduction; flow control; stochastically forced Navier-Stokes equations; turbulence modeling.**

I. Introduction

Sensor-free flow control strategies are capable of reducing drag in turbulent flows; examples of these strategies include spanwise wall oscillations [1], riblets, and streamwise traveling waves [2], [3]. Recently, numerical simulations of turbulent channel flows were used to demonstrate that upstream traveling waves can provide sustained levels of drag that are lower than in the laminar flow [2]. These numerical simulations have provided motivation for the development of a model-based framework for designing traveling waves to control the onset of turbulence [4], [5]. Furthermore, the results of [4], [5] have recently been extended to turbulent channel flows subject to spanwise wall-oscillations [6]. Theoretical predictions obtained in [6] were able to capture the behavior of the controlled turbulent flow which was previously observed in high fidelity simulations [1]. In this paper, we utilize a similar computationally efficient model-based method to study the effects of streamwise traveling waves on turbulent channel flows. This is achieved by combining turbulence modeling with stochastically forced linearized dynamics to determine the effect of small amplitude traveling waves on skin-friction drag. Our approach is capable of identifying drag reducing trends in traveling waves with various control parameters. We use high fidelity numerical simulations as a means for verifying trustworthiness of our theoretical predictions.

Our presentation is organized as follows: in Section II, we present the governing equations along with the turbulent viscosity model; in Section III, we describe the procedure for determining an approximation to the turbulent mean velocity in flow with control using turbulent viscosity of the uncontrolled flow; in Section IV, we use linearized Navier-Stokes (NS) equations to obtain second-order statistics of velocity fluctuations in controlled flow and to show how they influence the turbulent viscosity and skin-friction drag; and finally, in Section IV-D, we demonstrate the utility of our method in capturing drag-reducing trends of streamwise traveling waves. We summarize our results in Section V.

Financial support from the National Science Foundation under CAREER Award CMMI-06-44793 and from the University of Minnesota Initiative for Renewable Energy and the Environment under Early Career Award RC-0014-11 is gratefully acknowledged. The University of Minnesota Supercomputing Institute is acknowledged for providing computing resources.

A. Zare, B. K. Lieu, and M. R. Jovanović are with the Department of Electrical and Computer Engineering, University of Minnesota, Minneapolis (e-mails: arminzare@umn.edu, lieux006@umn.edu, mihailo@umn.edu).

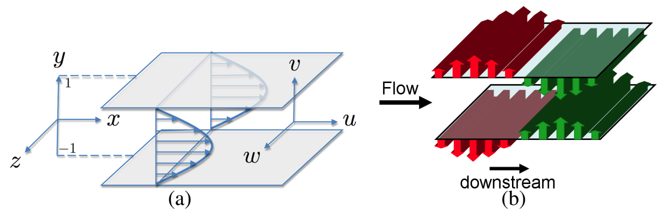

Fig. 1. (a) Pressure driven channel flow. (b) Boundary actuation of blowing and suction along the walls.

II. Problem formulation

A. Governing equations

We consider a three-dimensional turbulent channel flow of an incompressible viscous Newtonian fluid; see Fig. 1(a) for geometry. The flow is driven by a pressure gradient and is governed by the NS and continuity equations

$$\begin{aligned} \mathbf{u}_t &= -(\mathbf{u}\cdot\nabla)\mathbf{u} - \nabla P + (1/R_\tau)\,\Delta\mathbf{u}, \\ 0 &= \nabla\cdot\mathbf{u}, \end{aligned} \tag{1}$$

where $\mathbf{u}$ is the velocity vector, P is the pressure, ∇ is the gradient, $\Delta = \nabla\cdot\nabla$ is the Laplacian. The streamwise, wall-normal, and spanwise coordinates are represented by $\bar{x}$, $\bar{y}$, and $\bar{z}$, and time is denoted by $\bar{t}$. Equation (1) has been non-dimensionalized by scaling spatial coordinates with the channel half-height h, velocity with the friction velocity $u_\tau = \sqrt{\tau_w/\rho}$, time with inertial time scale h/u_τ, and pressure with ρu_τ^2. The important parameter in (1) is the friction Reynolds number, $R_\tau = u_\tau h/\nu$, which determines the ratio of inertial to viscous forces. Here, ρ is the fluid density and ν is the kinematic viscosity.

In addition to pressure gradient, the flow with control is subject to a zero-net-mass-flux surface blowing and suction. This imposes the following boundary conditions on the velocity fields,

$$\mathbf{u}\,(\bar{x},\bar{y}=\pm 1,\bar{z},\bar{t}) = [\,0 \;\; \mp 2\,\alpha\cos\left(\omega_x(\bar{x}-c\,\bar{t})\right) \;\; 0\,]^T, \tag{2}$$

978-1-4673-2066-5/12/$31.00 ©2012 IEEE

where ω_x, c, and α denote the frequency, speed, and amplitude of the traveling wave. Positive (negative) values of c define a wave that travels in the downstream (upstream) direction. We can eliminate the time dependence in (2) using a simple coordinate transformation, $(x = \bar{x} - c\bar{t},\ y = \bar{y},\ z = \bar{z},\ t = \bar{t})$, which adds an additional convective term to (1)

$$\begin{aligned} \mathbf{u}_t &= c\,\mathbf{u}_x - (\mathbf{u}\cdot\nabla)\,\mathbf{u} - \nabla P + (1/R_\tau)\,\Delta\mathbf{u}, \\ 0 &= \nabla\cdot\mathbf{u}. \end{aligned} \tag{3}$$

B. Navier-Stokes equations augmented with turbulent viscosity

Following a similar procedure as in [6], we augment the molecular viscosity in (3) with turbulent viscosity ν_T

$$\begin{aligned} \mathbf{u}_t &= c\,\mathbf{u}_x - (\mathbf{u}\cdot\nabla)\,\mathbf{u} - \nabla P + \\ &\quad (1/R_\tau)\,\nabla\cdot\left((1+\nu_T)\left(\nabla\mathbf{u} + (\nabla\mathbf{u})^T\right)\right), \\ 0 &= \nabla\cdot\mathbf{u}. \end{aligned} \tag{4}$$

This model has been used in [6] for model-based design of transverse wall oscillations for the purpose of drag reduction. Moarref and Jovanović [6] showed that this model is capable of capturing the essential features of the turbulent flow with control that were previously observed in high fidelity numerical simulations.

In order to determine the influence of traveling waves on skin-friction drag we need to develop robust models for approximating the turbulent viscosity, ν_T, in the presence of control. Several studies [7]–[9] have attempted to find expressions for ν_T that yield the turbulent mean velocity in flows without control. For example, the following model for the turbulent viscosity was developed in [9],

$$\begin{aligned} \nu_{T0}(y) &= \frac{1}{2}\left(\left(1 + \left(\frac{c_2}{3}\,R_\tau\,(1-y^2)\,(1+2y^2)\,\times \right.\right.\right. \\ &\qquad \left.\left.\left.(1 - e^{-(1-|y|)\,R_\tau/c_1})\right)^2\right)^{1/2} - 1\right) \end{aligned} \tag{5}$$

where the parameters c_1 and c_2 are selected to minimize least squares deviation between the mean streamwise velocity obtained with $\tau_w = 1$ and turbulent viscosity (5), and the mean streamwise velocity obtained in experiments and simulations.

Our model-based design of streamwise traveling waves for drag reduction involves two tasks:

(i) [Section III] **Mean flow analysis:** *assuming that* (5) *reliably approximates turbulent viscosity in the controlled flow, we determine the turbulent mean velocity in the flow subject to traveling waves*;

(ii) [Section IV] **Fluctuation dynamics:** *we quantify the effect of fluctuations around the mean velocity determined in (i) on turbulent viscosity and drag reduction*.

In Section III, we use perturbation analysis to determine the steady-state solution to (4) with turbulent viscosity given by (5) in the presence of small-amplitude boundary actuation (2). Using high-fidelity simulations of nonlinear flow dynamics we show that this approximation to turbulent mean velocity does not reliably predict the drag reducing effects of streamwise traveling waves. In Section IV, we then demonstrate that predictive capability of our analysis can be improved by examining stochastically-forced linearization of system (4)-(5) around its steady-state solution.

III. Turbulent mean velocity in flow with ν_{T0}

The first step in our analysis requires determination of an approximation to the turbulent mean velocity,

$$\mathbf{U} = \left[\ U(x,y)\quad V(x,y)\quad 0\ \right]^T,$$

in the presence of blowing and suction along the walls. This is achieved by finding the steady-state solution to (4)-(5),

$$\begin{aligned} 0 &= c\,\mathbf{U}_x - (\mathbf{U}\cdot\nabla)\,\mathbf{U} - \nabla P + \\ &\quad (1/R_\tau)\,\nabla\cdot\left((1+\nu_{T0})\left(\nabla\mathbf{U} + (\nabla\mathbf{U})^T\right)\right), \\ 0 &= \nabla\cdot\mathbf{U}, \end{aligned} \tag{6}$$

with boundary conditions

$$V(x, y = \pm 1) = \mp 2\,\alpha\cos(\omega_x\,x),\quad U(x,\pm 1) = 0. \tag{7}$$

For small amplitude actuation, $\alpha \ll 1$, a perturbation analysis can be employed to solve (6) subject to (7) and determine the corrections to the mean velocities,

$$\begin{aligned} U(x,y) &= U_0(y) + \alpha\,U_1(x,y) + \alpha^2\,U_2(x,y) + \mathcal{O}(\alpha^3), \\ V(x,y) &= \alpha\,V_1(x,y) + \alpha^2\,V_2(x,y) + \mathcal{O}(\alpha^3). \end{aligned} \tag{8}$$

Here, $U_0(y)$ represents the base velocity in the uncontrolled turbulent flow and it is determined from the solution to

$$\begin{aligned} 0 &= (1+\nu_{T0})\,U_0'' + \nu_{T0}'\,U_0' + R_\tau, \\ 0 &= U_0(y = \pm 1), \end{aligned} \tag{9}$$

where prime denotes differentiation with respect to the wall-normal coordinate y. Higher harmonics of the mean velocity can be represented as

$$\begin{aligned} U_1(x,y) &= U_{1,-1}(y)\,\mathrm{e}^{-\mathrm{i}\omega_x x} + U_{1,1}(y)\,\mathrm{e}^{\mathrm{i}\omega_x x}, \\ V_1(x,y) &= V_{1,-1}(y)\,\mathrm{e}^{-\mathrm{i}\omega_x x} + V_{1,1}(y)\,\mathrm{e}^{\mathrm{i}\omega_x x}, \\ U_2(x,y) &= U_{2,0}(y) + U_{2,-2}(y)\,\mathrm{e}^{-2\mathrm{i}\omega_x x} + U_{2,2}(y)\,\mathrm{e}^{2\mathrm{i}\omega_x x}, \\ V_2(x,y) &= V_{2,-2}(y)\,\mathrm{e}^{-2\mathrm{i}\omega_x x} + V_{2,2}(y)\,\mathrm{e}^{2\mathrm{i}\omega_x x}. \end{aligned}$$

Under the assumption of the fixed bulk,

$$\int_{-1}^{1} \overline{U(x,y)}\,\mathrm{d}y = \int_{-1}^{1} U_0(y)\,\mathrm{d}y,$$

the skin-friction drag is determined by the slope of the streamwise mean velocity at the walls,

$$D = \frac{1}{2}\left(\left.\frac{\mathrm{d}\overline{U}}{\mathrm{d}y}\right|_{-1} - \left.\frac{\mathrm{d}\overline{U}}{\mathrm{d}y}\right|_{1}\right), \tag{10}$$

where the overline denotes the average value obtained by integration in the x-direction. Thus, up to a second-order in

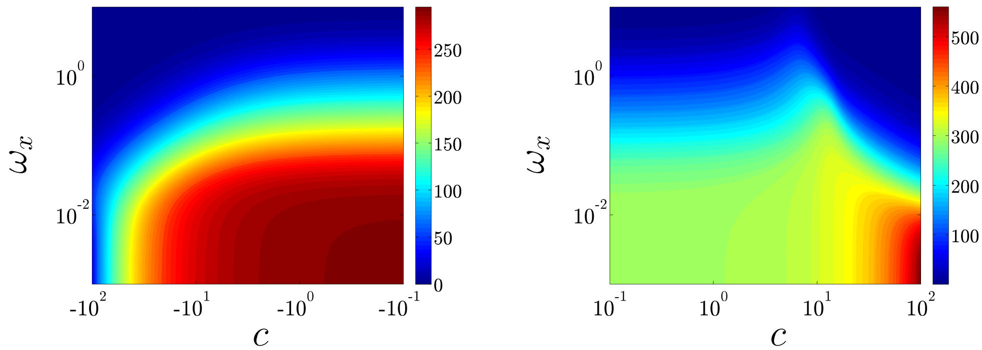

(a) (b)

Fig. 2. Second-order correction to the skin-friction drag D_2 as a function of traveling wave speed c and frequency ω_x: (a) upstream traveling waves; and (b) downstream traveling waves. Predictions are obtained using the solution to (6)-(7) with turbulent viscosity determined by (5).

α, the only terms that influence D are U_0 and $U_{2,0}$,

$$\begin{aligned} D &= D_0 + \alpha^2 D_2 + \mathcal{O}(\alpha^4), \\ D_0 &:= (U_0'(-1) - U_0'(1))/2, \\ D_2 &:= (U_{2,0}'(-1) - U_{2,0}'(1))/2, \end{aligned}$$

Figure 2 shows the second order correction to skin-friction drag D_2, as a function of the traveling wave speed and frequency. We observe that both upstream and downstream traveling waves increase drag. This is in contrast to the results obtained using simulations of the nonlinear flow dynamics [2], [5] where it was shown that drag reduction can be obtained for certain values of traveling wave parameters. For an upstream traveling wave with $c = -2$ and $\omega_x = 0.5$, Fig. 3 also demonstrates increase in drag for all values of the wave amplitude α. We observe close correspondence between the results obtained from the solution to (6)-(7) with ν_{T0} determined by (5) using terms up to a second order in α, fourth order in α, and Newton's method.

The results of this section show the inability of the above conducted mean flow analysis to capture the drag reducing effects of streamwise traveling waves. In Section IV, we demonstrate that the gap between our predictions and the results of high-fidelity numerical simulations can be significantly reduced by analyzing the dynamics of fluctuations around the mean velocity profile determined here.

IV. Dynamics of velocity fluctuations

In this section, we examine the dynamics of fluctuations around the turbulent mean profile $\mathbf{U}$ determined in Section III. The second-order statistics of the flow with control are obtained using stochastically-forced NS equations. For small amplitude actuation, we employ perturbation analysis to determine turbulent viscosity and the resulting correction to the skin-friction drag from these statistics.

A. Linearized Navier-Stokes equations

The dynamics of infinitesimal velocity fluctuations $\mathbf{v} = \begin{bmatrix} u & v & w \end{bmatrix}^T$ around the turbulent mean velocity $\mathbf{U}$ are governed by

$$\begin{aligned} \mathbf{v}_t &= c\,\mathbf{v}_x - (\mathbf{U}\cdot\nabla)\,\mathbf{v} - (\mathbf{v}\cdot\nabla)\,\mathbf{U} - \nabla p + \mathbf{f} \\ &\quad + (1/R_\tau)\nabla\cdot\left((1+\nu_{T0})\left(\nabla\mathbf{v} + (\nabla\mathbf{v})^T\right)\right), \\ 0 &= \nabla\cdot\mathbf{v}. \end{aligned} \tag{11}$$

Equation (11) is driven by zero-mean temporally white stochastic forcing $\mathbf{f}$. Since the boundary conditions (2) are satisfied by turbulent mean velocity, the velocity fluctuations $\mathbf{v}$ assume no-slip boundary conditions. Following a similar procedure as in [4], we can bring the set of spatially periodic PDEs (11) into the following evolution form

$$\begin{aligned} \partial_t\boldsymbol{\psi}_\theta(y,k_z,t) &= A_\theta(k_z)\,\boldsymbol{\psi}_\theta(y,k_z,t) + \mathbf{f}_\theta(y,k_z,t), \\ \mathbf{v}_\theta(y,k_z,t) &= C_\theta(k_z)\,\boldsymbol{\psi}_\theta(y,k_z,t), \end{aligned} \tag{12}$$

where $\boldsymbol{\psi} = [\,v \quad \eta\,]^T$ is the state vector with $\eta = \partial_z u - \partial_x w$ being the wall-normal vorticity. Homogenous Dirichlet boundary conditions are imposed on η, while homogeneous Dirichlet and Neumann boundary conditions are imposed on v.

We note that $\boldsymbol{\psi}$, $\mathbf{v}$, and $\mathbf{f}$ are bi-infinite column vectors parameterized by θ and k_z, e.g., $\boldsymbol{\psi}_\theta(y,k_z,t) = \mathrm{col}\{\boldsymbol{\psi}(\theta_n,y,k_z,t)\}_{n\in\mathbb{N}}$. Furthermore, for each θ and k_z, $A_\theta(k_z)$ and $C_\theta(k_z)$ are bi-infinite matrices whose elements are integro-differential operators in y. The operator A_θ can be written as $A_\theta = A_{0\theta} + \sum_{\ell=1}^{\infty}\alpha^\ell A_{\ell\theta}$ where the definition of $A_{\ell\theta}$ can be found in [4]. In the next section, we exploit the structure of the operator A_θ and use perturbation analysis to determine the auto-correlation operator of $\boldsymbol{\psi}_\theta$ for small values of the traveling wave amplitude, α.

B. Second-order statistics of velocity fluctuations

Consider the linearized system (12) driven by zero-mean temporally white stochastic forcing with second-order statistics,

$$\mathcal{E}\left(\mathbf{f}(\,\cdot\,\boldsymbol{\kappa},t_1)\otimes\mathbf{f}(\,\cdot\,,\boldsymbol{\kappa},t_2)\right) = M(\boldsymbol{\kappa})\,\delta(t_1 - t_2).$$

Here, $\boldsymbol{\kappa} = (\theta, k_z)$ denotes the wave-numbers, δ is the Dirac delta function, $\mathbf{f}\otimes\mathbf{f}$ is the tensor product of $\mathbf{f}$ with itself, and

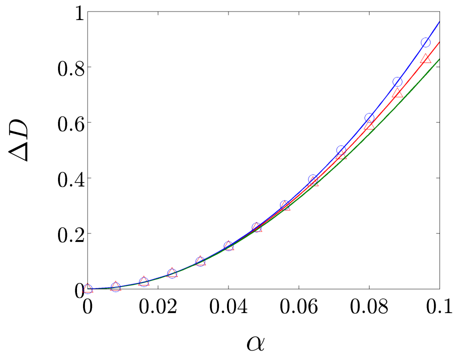

Fig. 3. Drag variation, $\Delta D = D - D_0$, as a function of wave amplitude α for an upstream traveling wave with $c = -2$ and $\omega_x = 0.5$. Predictions are obtained from the solution to (6)-(7) with turbulent viscosity determined by (5) using terms up to a second order in α ($\circ$), fourth order in α ($\triangledown$), and Newton's method (solid curve).

$M(\boldsymbol{\kappa})$ is the spatial spectral-density of forcing. We follow [6] and select M so that the two-dimensional energy spectra of the stochastically forced linearized NS equations match those of the uncontrolled turbulent flow. For this purpose, we use the energy spectrum of the uncontrolled flow $E(y, \boldsymbol{\kappa})$ resulting from numerical simulations of the nonlinear flow dynamics [10], [11] to define

$$M(\boldsymbol{\kappa}) = \frac{\bar{E}(\boldsymbol{\kappa})}{\bar{E}_0(\boldsymbol{\kappa})}\, M_0(\boldsymbol{\kappa}),$$

$$M_0(\boldsymbol{\kappa}) = \begin{bmatrix} \sqrt{E}\, I & 0 \\ 0 & \sqrt{E}\, I \end{bmatrix} \begin{bmatrix} \sqrt{E}\, I & 0 \\ 0 & \sqrt{E}\, I \end{bmatrix}^{+},$$

where $\bar{E}(\boldsymbol{\kappa}) = (1/2) \int_{-1}^{1} E(y, \boldsymbol{\kappa})\, \mathrm{d}y$ represents the two-dimensional energy spectrum of the uncontrolled flow and $\bar{E}_0$ is the energy spectrum obtained from the linearized NS equations subject to white-in-time forcing with spatial spectrum $M_0(\boldsymbol{\kappa})$. The $^+$ sign denotes the adjoint of an operator which should be determined with respect to the appropriate inner product; for additional details see [12].

For the linearized system (12), the steady-state auto-correlation operator of $\boldsymbol{\psi}_\theta$ can be determined from the solution to the Lyapunov equation,

$$A_\theta(k_z)\mathcal{X}_\theta(k_z) \,+\, \mathcal{X}_\theta(k_z)A_\theta^{+}(k_z) \,+\, M_0(\theta, k_z) = 0,$$

and the energy spectrum is given by

$$E_0(\boldsymbol{\kappa}) = \mathrm{trace}(\mathcal{X}_\theta(k_z)) = \sum_{n=-\infty}^{\infty} \mathrm{trace}(X_d(\theta_n, k_z)),$$

where $X_d(\theta_n, k_z)$ represents the elements on the main diagonal of $\mathcal{X}_\theta$. For small amplitude actuation, perturbation analysis in conjunction with the special structure of the operator A_θ can be used to express $\mathcal{X}_\theta(k_z)$ as

$$\mathcal{X}_\theta(k_z) \;=\; \mathcal{X}_{\theta,0}(k_z) \,+\, \alpha^2\, \mathcal{X}_{\theta,2}(k_z) \,+\, \mathcal{O}(\alpha^4),$$

where $\mathcal{X}_{\theta,0}(k_z)$ and $X_{\theta,2}(k_z)$ are solutions to a set of coupled operator-valued Lyapunov and Sylvester equations [13]. The auto-correlation operator $\mathcal{X}_{\theta,0}(k_z)$ contains the contribution of the flow with no control, and $X_{\theta,2}(k_z)$ captures the effect of control (up to second-order in α).

C. Influence of fluctuations on turbulent viscosity and skin-friction drag

We next show how velocity fluctuations in the flow with control introduce a second order correction to turbulent viscosity and skin-friction drag. We use the kinetic energy of velocity fluctuations, k, and its rate of dissipation, ϵ, to determine the influence of fluctuation on the turbulent viscosity,

$$\nu_T \;=\; C_\mu\, R_\tau^2 \left(k^2/\epsilon\right), \tag{13}$$

where $C_\mu = 0.09$ is a model constant. Both k and ϵ are determined by the second-order statistics of velocity fluctuations,

$$\begin{aligned} k(y) \;&=\; (1/2)\; (\overline{uu} + \overline{vv} + \overline{ww})\,, \\ \epsilon(y) \;&=\; 2\,(\overline{u_x\, u_x} \,+\, \overline{v_y\, v_y} \,+\, \overline{w_z\, w_z} \,+\, \overline{u_y\, v_x} \\ &\quad +\overline{u_z\, w_x} \,+\, \overline{v_z\, w_y}) \,+\, \overline{u_y\, u_y} \,+\, \overline{w_y\, w_y} \\ &\quad +\overline{v_x\, v_x} \,+\, \overline{w_x\, w_x} \,+\, \overline{u_z\, u_z} \,+\, \overline{v_z\, v_z}. \end{aligned} \tag{14}$$

The overline in (14) denotes averaging in the streamwise and spanwise directions.

In the flow subject to small amplitude traveling waves, k and ϵ can be expressed as

$$\begin{aligned} k \;&=\; k_0 \,+\, \alpha^2\, k_2 \,+\, \mathcal{O}(\alpha^4), \\ \epsilon \;&=\; \epsilon_0 \,+\, \alpha^2\, \epsilon_2 \,+\, \mathcal{O}(\alpha^4), \end{aligned} \tag{15}$$

where the subscript 0 denotes the corresponding quantities in the uncontrolled flow, and the subscript 2 denotes the influence of fluctuations at the level of α^2.

By substituting (15) into (13) and applying the Neumann series expansion we obtain an expression that establishes the dependence of the second-order correction to ν_T on k_2 and ϵ_2,

$$\begin{aligned} \nu_T \;&=\; \nu_{T0} \,+\, \alpha^2\, \nu_{T2} \,+\, \mathcal{O}(\alpha^4), \\ \nu_{T2} \;&=\; \nu_{T0} \left(\frac{2k_2}{k_0} \,-\, \frac{\epsilon_2}{\epsilon_0} \right). \end{aligned} \tag{16}$$

The influence of fluctuations on turbulent mean velocity (and consequently the skin-friction drag) can be obtained by substituting ν_T from (16) into (4) and finding the resulting steady-state solution.

D. Results: turbulent drag reduction and net efficiency

We next examine the effect of an upstream traveling wave with $c = -2$ and $\omega_x = 0.5$ on the skin-friction drag in a turbulent channel flow with $R_\tau = 186$. For this choice of traveling wave parameters, numerical simulations of nonlinear flow dynamics at $R_\tau \approx 63$ have demonstrated the drag-reducing ability of upstream traveling waves [2], [5].

Figure 4 shows the time dependence of the skin-friction drag for the uncontrolled turbulent flow and for the flow subject to an upstream traveling wave with $c = -2$, $\omega_x = 0.5$, and two wave amplitudes ($\alpha = 0.01$ and $\alpha = 0.05$). The

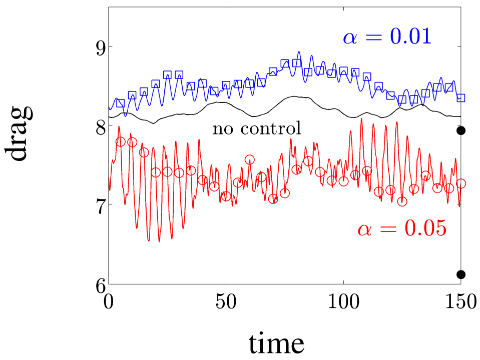

Fig. 4. Drag in a turbulent channel flow obtained from high-fidelity simulations with $R_\tau = 186$ subject to an upstream traveling wave ($c = -2$, $\omega_x = 0.5$) at two wave amplitudes, $\alpha = 0.01$ (□) and $\alpha = 0.05$ (○). The black dots denote the drag computed using the model-based framework of Section IV.

solid lines are obtained using simulations of the nonlinear NS equations, and the black dots indicate the corresponding steady-state values of drag resulting from the model-based approach of Section IV. Compared to the flow with no control, from Fig. 4 it appears that the traveling wave with $\alpha = 0.01$ slightly increases drag. However, numerical simulation conducted over longer time horizon (not shown here) indicates a very small discrepancy between the uncontrolled flow results and the results obtained for the upstream traveling wave with $\alpha = 0.01$. For $\alpha = 0.05$, our results (obtained using perturbation analysis up to second-order in α) suggest that the upstream traveling waves should be able to reduce drag. Even though this prediction is verified in numerical simulations of the nonlinear NS equations (see red curve in Fig. 4), we observe a mismatch between numerically obtained values of the drag and those resulting from our analysis. We are currently in the process of testing whether this mismatch can be reduced by accounting for the higher order corrections to the turbulent viscosity in our perturbation analysis.

V. Concluding Remarks

We have developed a model-based framework to design streamwise traveling waves for drag reduction in a turbulent channel flow. Our approach consists of two steps: (1) we use the turbulent viscosity of the uncontrolled flow to approximate the influence of control on the turbulent mean velocity; and (2) we use second-order statistics of stochastically forced equations linearized around this mean profile to examine the influence of velocity fluctuations on the turbulent viscosity and skin-friction drag. We demonstrate that the mean flow analysis alone is not capable of capturing the essential drag-reducing trends of streamwise traveling waves. In order to improve quality of prediction, we need to incorporate the influence of fluctuations on the turbulent viscosity and skin-friction drag. For an upstream traveling wave with $c = -2$ and $\omega_x = 0.5$ we have employed perturbation analysis in the traveling wave amplitude to demonstrate that analysis of dynamics can reduce the gap between theoretical predictions and results of high-fidelity numerical simulations. Our ongoing effort is focused on incorporating higher order corrections to the turbulent viscosity and on studying the mechanisms responsible for turbulent drag reduction.

Acknowledgments

The authors would like to thank Rashad Moarref for useful discussion.

References

[1] M. Quadrio and P. Ricco, "Critical assessment of turbulent drag reduction through spanwise wall oscillations," *J. Fluid Mech.*, vol. 521, pp. 251–271, 2004.

[2] T. Min, S. Kang, J. Speyer, and J. Kim, "Sustained sub-laminar drag in a fully developed channel flow," *J. Fluid Mech.*, vol. 558, pp. 309–318, 2006.

[3] J. Hœpffner and K. Fukagata, "Pumping or drag reduction?" *J. Fluid Mech.*, vol. 635, pp. 171–187, 2009.

[4] R. Moarref and M. R. Jovanović, "Controlling the onset of turbulence by streamwise traveling waves. Part 1: Receptivity analysis," *J. Fluid Mech.*, vol. 663, pp. 70–99, November 2010.

[5] B. K. Lieu, R. Moarref, and M. R. Jovanović, "Controlling the onset of turbulence by streamwise traveling waves. Part 2: Direct numerical simulations," *J. Fluid Mech.*, vol. 663, pp. 100–119, November 2010.

[6] R. Moarref and M. R. Jovanović, "Model-based design of transverse wall oscillations for turbulent drag reduction," *J. Fluid Mech.*, vol. 707, pp. 205–240, September 2012.

[7] W. V. R. Malkus, "Outline of a theory of turbulent shear flow," *J. Fluid Mech.*, vol. 1, no. 5, pp. 521–539, 1956.

[8] R. D. Cess, "A survey of the literature on heat transfer in turbulent tube flow," *Westinghouse Research, Rep. 8-0529-R24*, 1958.

[9] W. C. Reynolds and W. G. Tiederman, "Stability of turbulent channel flow with application to Malkus's theory," *J. Fluid Mech.*, vol. 27, no. 2, pp. 253–272, 1967.

[10] J. C. Del Alamo and J. Jimenez, "Spectra of the very large anisotropic scales in turbulent channels," *Phys. Fluids*, vol. 15, no. 6, pp. 41–44, 2003.

[11] J. Del Alamo, J. Jiménez, P. Zandonade, and R. Moser, "Scaling of the energy spectra of turbulent channels," *J. Fluid Mech.*, vol. 500, no. 1, pp. 135–144, 2004.

[12] M. R. Jovanović and B. Bamieh, "Componentwise energy amplification in channel flows," *J. Fluid Mech.*, vol. 534, pp. 145–183, July 2005.

[13] M. Fardad and B. Bamieh, "Perturbation methods in stability and norm analysis of spatially periodic systems," *SIAM J. Control Optim.*, vol. 47, pp. 997–1021, 2008.